Journal of the Serbian Chemical Society
JSCS-info@shd.org.rs • www.shd.org.rs/JSCS
J. Serb. Chem. Soc. *90* (3) 339–350 (2025)
JSCS–5391
Original scientific paper
Published 24 March, 2025

Coating technology on mortar surface for extending service life of on-site building construction

NIDCHAMON JUMRUS[1,2], MONWIPA THAPINTA[2], PATCHARAPORN CHAIWONG[2], ARISARA PANTAWAN[1,2], TEWASIN KUMPIKA[2], WINAI THONGPAN[3], NIWAT JHUNTAMA[4], EKKAPONG KANTARAK[2], WATTIKON SROILA[2], RATTIYAKORN RIANYOI[2], PISITH SINGJAI[2] and WIRADEJ THONGSUWAN[2]*

[1]Office of Research Administration, Chiang Mai University, Chiang Mai 50200, Thailand, [2]Department of Physics and Materials Science, Faculty of Science, Chiang Mai University, Chiang Mai, 50200, Thailand, [3]Department of Physics, Faculty of Science and Technology, Thammasat University, Lampang, 52190, Thailand and [4]Faculty of Science and Agricultural Technology, Rajamangala University of Technology Lanna, Chiang Mai 50300, Thailand

(Received 17 April, revised 24 May, accepted 25 August 2024)

Abstract: The superhydrophobic, self-cleaning and anti-corrosion surface was successfully coated on mortar using an effective one-step spray coating technique. A coating solution was prepared by mixing methyltrichlorosilane-modified SiO_2/TiO_2 nanoparticles at different ratios to enhance the superhydrophobicity and reduce water absorption of the mortar. The sample prepared using a SiO_2/TiO_2 with the ratio of 75/25 was found to be optimal, exhibiting a high water contact angle and low sliding angle, which resulted in a reduction of water absorption by more than 97.5 % and chloride ion penetration depth. Furthermore, the robustness of the superhydrophobic coating was analyzed against various tests including water drop impact, sand abrasion impact, tape peeling and sandpaper abrasion tests, each test was conducted with over 10000 drops, 300 g, 60 cycles and 5 cycles, respectively. Notably, the coating showed excellent water absorption reduction of 82.6 % after sandpaper abrasion for a length of 200 cm (20 cycles), even though the water contact angle was reduced to 118°. Thus, the fabrication of superhydrophobic mortar surface offers a novel, alternative approach that is simple, efficient, cost-effective and provides multifunction protection surface to increase the service life of on-site building construction with enhanced mechanical durability and anti-corrosion properties.

Keywords: superhydrophobic; methyltrichlorosilane; self-cleaning; mechanical durability; anti-corrosion.

* Corresponding author. E-mail: wiradej.t@cmu.ac.th
https://doi.org/10.2298/JSC240417080J

INTRODUCTION

Mortars are widely used in the construction industry due to their versatility and cost-effectiveness.[1] However, their susceptibility to water and corrosive ions such as Cl^-, SO_4^{2-}, *etc*., leads to the physical and chemical degradation processes.[2] The concrete structure may crack, spall and delaminate and steel bars in the buildings can be affected by chloride corrosion, leading to the strength reduction. Therefore, it is essential to limit water penetration and enhance anti-corrosion properties to improve durability and prolong the service life of building structures.[3]

Surface superhydrophobicity is one of the methods for creating new functional materials with complete waterproof,[4] self-cleaning[5] and anti-corrosion properties.[6] It is well known that a surface is considered superhydrophobic when it exhibits a water contact angle (WCA) greater than 150° and a sliding angle (SA) less than 10°. Artificial superhydrophobic coatings can be achieved by creating hierarchical surface morphology and modifying it with low surface energy materials.[7] Recently, SiO_2 and TiO_2 nanoparticles (NPs) along with various alkyl silanes have been used to create superhydrophobic coatings such as butyltrichlorosilane (BTS), octadecyltrichlorosilane (ODTS) and methyltrichlorosilane (MTCS).[8,9] MTCS is one of the alkyltrichlorosilanes (trichlorosilane head group with a hydrocarbon tail group of variable length) that has the shortest chain lengths and higher reactivity than others. It can facilitate the polycondensation reactions at room temperature.[9,10] In recent years, many researchers have studied bulk composite superhydrophobic cement mortar to extend the service life in construction.[1–3] However, the composites high-cost is due to a lot of starting materials, which may impact the mechanical properties (compressive strength and flexural strength).

This study aims to replace bulk composites with a simple spray coating technique using MTCS-modified SiO_2/TiO_2 NPs on mortar surface. The coating offers the advantage of easy application on-site building construction unaffecting the structure, resulting in time and cost savings. Additionally, it effectively prevents water and corrosive ions from penetrating into the inner spaces of buildings as well as bulk composites. The ratio SiO_2/TiO_2 NPs was optimized to increase surface roughness, reduce surface energy, and enhance water permeability resistance. Furthermore, the superhydrophobic mortar demonstrates excellent self-cleaning, mechanical durability and anti-corrosion properties. This work presents a novel alternative coating methodology for creating durable superhydrophobic on mortar surfaces, instead of the composites superhydrophobic cement mortar.

EXPERIMENTAL

Preparation of superhydrophobic mortar

First, Portland cement (The Siam Public Company Ltd.) was mixed with water at a ratio of 5:1. Then, the mixed mortar was placed into oiled molds (2 cm diameter and 0.6 cm thick).

After that, the mortars were removed from the molds and cured for 7 days before testing. To prepare the superhydrophobic coating, a solution was created by adding 0.8 % of fumed silica (SiO_2, 7 nm, Sigma–Aldrich Pte. Ltd.) and titanium dioxide (TiO_2, 21 nm, Ajax Finechem) with ratios of 0/100, 25/75, 50/50, 75/25 and 100/0 to methyltrichlorosilane (MTCS, 99.5 % purity, Sigma–Aldrich Pte. Ltd.) dissolved in toluene (99.5 % purity, RCI Labscan Ltd.) at a concentration of 2.5 vol. %. The mixture solution was stirred for 1 h and then sprayed onto the mortar surface using a spray coating technique for 15 times. The spray gun was held perpendicular to the surface at a distance of 10 cm under ambient air and atmospheric pressure.

Characterizations

The surface morphology and porosity of samples were analyzed using scanning electron microscopy (SEM, Hitachi TM4000Plus) and ImageJ software. The chemical bonding was analyzed using Fourier-transform infrared spectrometry (FTIR, BurkerTENSOR 27) and X-ray diffraction (XRD, Rigaku Smartlab) on the surface of uncoated and coated samples with the size of 2 cm in diameter and 0.6 cm thick. Water contact angles (WCA) and sliding angles (*SA*) were measured using a pendant drop tensiometer with 3 μL of deionized water. The permeability of water was evaluated by measuring the rate of water absorption by dry specimen mortar in 1 h.

Mechanical durability tests

The mechanical durability of the coating surface was evaluated through water drop impact test, sand abrasion impact test, tape peeling test and sandpaper abrasion test. For the water drop impact test, water droplet of 40 μL was dropped onto the superhydrophobic mortar surface from a height of 10 cm and a tilt angle of 45°. The sand abrasion impact test involved impacting grains of sizes 100–500 μm on the surfaces at a height 40 cm and a tilt angle of 45° with a flow rate of 2.8 m s^{-1}. The tape peeling test was carried out using the method reported in ASTM D3359-09.[11] The coating mortar surface was pressed with 3M tape under a pressure of 3 kPa to ensure good contact between the surface and the 3M tape. Then, the tape was peeled off from the surface and the above process was repeated. The sandpaper abrasion test was performed on the superhydrophobic mortar surface using sandpaper grit No. 600 as the abrasion surface. The sample was moved in one direction for 10 cm at a speed of 5 mm s^{-1} with a load of 100 g. The WCAs after mechanical durability tests were then investigated.

Chloride permeability test

The mortar samples were covered by epoxy resin (World Chemical Far East Company Ltd.) except for the diffusion surface. Then, the samples were soaked in a 7 wt. % NaCl (Labscan Asia Co., Ltd.) solution for 14 days. After that, a 0.1 mol/L silver nitrate ($AgNO_3$, RCI Labscan Ltd.) solution was sprayed on the cut surface.[3] The depth of chloride ion penetration was measured using the $AgNO_3$ color development test.

RESULTS AND DISCUSSION

Morphology analysis

The morphology of ordinary mortar (OM) and mortars coated with MTCS-modified SiO_2/TiO_2 nanoparticles (NPs) after 15 spraying times were analyzed in detail, using SEM. Fig. 1a shows the hydration products with rough and highly porous surface of the mortar (19.2 %). After spraying, the MTCS-modified SiO_2/TiO_2 coating covered the pore structure of the mortar, as shown in Fig. 1b–f.

From the figure, the porosity of the coated surface (which was measured using ImageJ)[12] decreased to 10.2, 8.5, 6.9, 8.6 and 6.1 %, respectively. The surface of the MTCS-modified TiO_2 (0/100) coating consisted of large, loose agglomerates of TiO_2 (Fig. 1b) while the MTCS-modified SiO_2 (100/0) coating surface was densely packed (Fig. 1f). The size of TiO_2 particles approximately three times larger than that of SiO_2 particles, resulting in a dense and low-porosity SiO_2 film. However, superhydrophobic surface requires a hierarchical surface with mono--scale roughness, which was observed in the SiO_2/TiO_2 ratios of 25/75 and 75/25 (Fig 1c and e).

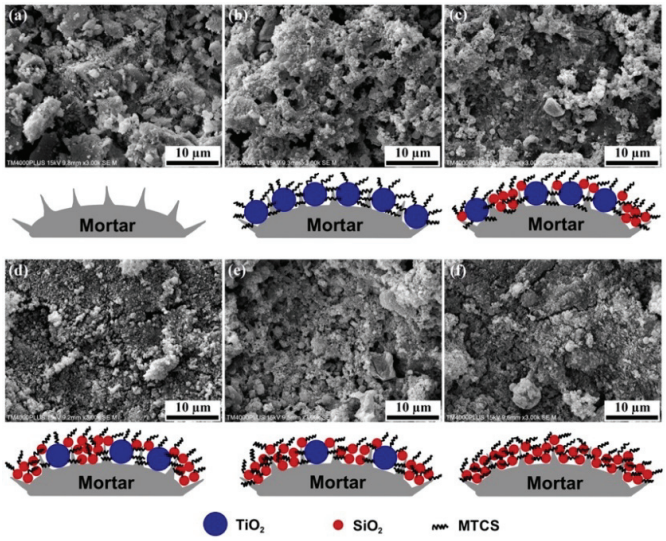

Fig. 1. Surface morphologies and schematic diagram of: a) ordinary mortar and the coated mortar by MTCS-modified SiO_2/TiO_2 NPs in ratios of b) 0/100, c) 25/75, d) 50/50, e) 75/25 and f) 100/0.

Wettability analysis

Fig. 2 shows water contact angle (WCA) of OM and coated mortar. The OM exhibited hydrophilicity with a WCA of 55.2°. After coating with MTCS-modified SiO_2/TiO_2 at different ratios using 15 spray applications, the mortar surfaces transformed into hydrophobic and superhydrophobic surfaces, with WCAs of 149.3, 145.6, 154.1, 154.7 and 145.7°, respectively. Interestingly, the samples coated at SiO_2/TiO_2 ratios of 50/50 and 75/25 displayed superhydrophobic mortar with WCA greater than 150° and SA less than 2°. Therefore, the hierarchical structure and low surface energy of the coated mortar surface contributed to the superhydrophobic behavior. This wetting behavior can be explained by the Cassie–Baxter equation:[13]

$$\cos\theta_\gamma = f_1\cos\theta - f_2 = f_1(\cos\theta + 1) - 1 \quad (1)$$

where θ_γ is the contact angle of the coated mortar surface, θ is the contact angle of the ordinary mortar surface (55.2°), f_1 is the solid fraction between the coated mortar and the droplet, f_2 is the air fraction between the coated mortar and the droplet. The solid fraction (f_1) and air fraction (f_2) of coated mortars are presented in Table I. The results imply that the ratio of SiO_2/TiO_2 increases air pockets in the rough structure, forming a solid-gas composition interface. Moreover, the smaller contact area between the droplet and coated mortar surface trends to increase the superhydrophobicity.

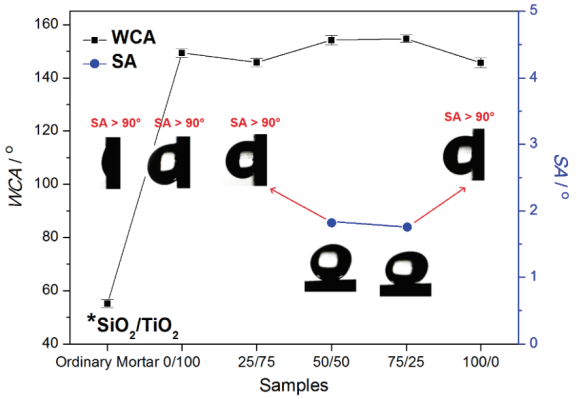

Fig. 2. Water contact angles and sliding angles of samples.

TABLE I. Solid fraction, air fraction and water permeability of ordinary and coated mortars

Sample	Solid fraction (f_1)	Air fraction (f_2)	Coefficient of water absorption, 10^{-9} cm^2 s^{-1}	Reduction in the coefficient of water absorption, %
OM	–	–	700	–
0/100	0.089	0.911	36.1	94.8
25/75	0.110	0.890	57.4	91.8
50/50	0.064	0.936	29.0	95.9
75/25 (SM)	0.061	0.939	17.7	97.5
100/0	0.111	0.889	74.5	89.4

Furthermore, water permeability property was measured by the coefficient of water absorption, as shown in Table I. The coefficient of water absorption value was calculated by the equation:[14]

$$K_a = (\frac{Q}{A})\frac{1}{t} \quad (2)$$

where K_a is the coefficient of water absorption, cm^2 s^{-1}; Q is the quantity of water absorbed by the sample, cm^3, in time, t / s and A is the total surface area of the sample, cm^2. For the OM, the coefficient of water absorption was measured

to be 700×10^{-9} cm^2 s^{-1}. After spraying, the coefficient of water absorption of all samples decreases by over 88 % compared to OM, indicating that the coating layer prevented water absorption into the pore structure of the mortar. Interestingly, the samples coated with MTCS-modified SiO_2/TiO_2 at a ratio of 75/25 exhibited the highest water resistance with a 97.5 % which reduced the coefficient of water absorption. This is because the appropriate combination between SiO_2 and TiO_2 increase the nano-scale roughness on the surfaces (see Fig. 1e) as well as the highest air fraction (see Table I). Air pockets between the water drops and surface prevent water absorption into the mortar surface, following the Cassie–Baxter model.[4] Therefore, MTCS-modified SiO_2/TiO_2 in a ratio of 75/25 is considered to have sufficient potential for practical applications due to hierarchical surface, high WCA and low water resistance, representing an optimum superhydrophobic mortar (SM) in this study. This result indicates that the coating of MTCS-modified SiO_2/TiO_2 NPs created a protective barrier on the mortar surface which improved the superhydrophobicity and effectively prevented the infiltration of water entering the mortar and causing damage. Therefore, this property is closely connected to the durability of mortar in outdoor environments, suggesting that the superhydrophobic coating can improve the service life and performance of the mortar in practical applications.

Chemical composition analysis

Fig. 3a displays the FTIR transmission spectra of ordinary mortar (OM) and superhydrophobic mortar (SM) with wavenumbers ranging from 4000 to 400 cm^{-1}. The absorption bands of OM at 435 cm^{-1} correspond to Si–O.[5] Peaks at 1400, 872 and 710 cm^{-1} are attributed to the C–O bond due to the presence of calcite in mortar.[15,16] The peaks at 1800–2300 cm^{-1} were observed in mortar.[17] The peak at 3643 cm^{-1} corresponds to the O–H vibration of portlandite ($Ca(OH)_2$).[5] After modification, the absorption band at 2970 cm^{-1} was attributed to the C–H bond in the $–CH_3$ group. Additionally, the peak 1271 cm^{-1} corresponded to the bending vibration of $Si–CH_3$, indicating successful MTCS modification and surface energy reduction.[18] In addition, the peaks at 1026 and 767 cm^{-1} belong to Si–O–Si,[5] which are consistent with the functional groups in the MTCS structure, forming a self-assembled film. TiO_2 NPs are approximately three times larger in diameter compared to SiO_2 nanoparticles while the specific surface area is less than SiO_2 NPs. Thus, the appropriate combination between SiO_2 and TiO_2 can increase specific surface area, leading to increase –OH groups. The superhydrophobic modification mechanism involved MTCS reacting with the –OH groups of SiO_2 and TiO_2 NPs through hydrolysis and condensation reactions, leading to the grafting of alkoxy groups of MTCS on the SiO_2 and TiO_2 surfaces.[4] Then, MTCS-modified SiO_2/TiO_2 NPs absorbed onto the mortar surface and filled lager pores of hydration products. Thus, the SiO_2/TiO_2 NPs reacted with MTCS

to reduce the surface energy and improve the surface roughness on mortar. The peaks at 1800–2300 cm^{-1} in SM were of very low intensity, indicating that the mortar surface is covered with a low surface energy coating. In Fig. 3b, the XRD pattern of OM and SM is presented. The main components of mortar are the same, namely calcite, quartz, portlandite, calcium silicate hydrate, alite and belite.[19] After coating, the SM shows lower intensity peaks of mortar, while significant peaks of SiO_2 and TiO_2 appeared.[20,21]

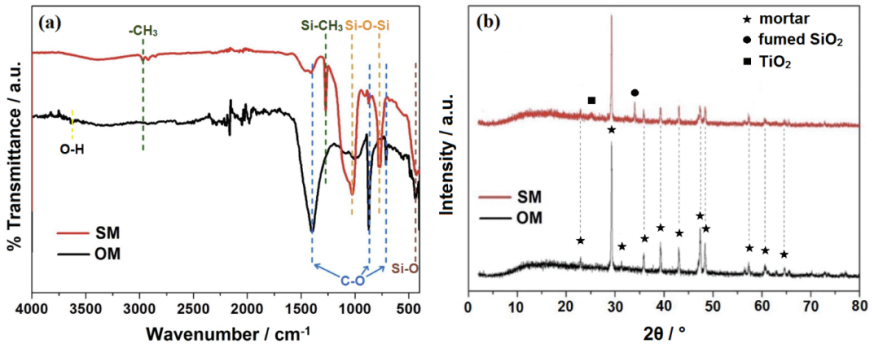

Fig. 3. a) The FTIR spectra and b) X-ray diffraction patterns of ordinary mortar (OM) and superhydrophobic mortar (SM).

Self-cleaning and mechanical durability properties

It is well known that outdoor mortar is easy to face with dust particles over time. The cumulation of pollutants for a long time will have a negative impact on the performance of mortars. The self-cleaning property of the OM and SM was tested using sand as a contaminator, as shown in Fig. 4a and b. In the SM, water droplets bead up into spheres and leave no residual droplets on the surface. This result indicated that the MTCS-modified SiO_2/TiO_2 NPs form a film on the mortar, exhibiting negligible water adhesion. Fig. 4c shows the mechanism of self-cleaning of the SM. While the water drop is rolling, it collects dust particles, demonstrating excellent self-cleaning property. In the Cassie–Baxter state, the droplet rests on top of the surface features, suspended by air pockets between the liquid droplet and the MTCS-modified SiO_2/TiO_2 NPs surfaces. These air pockets reduce the contract area, generating a greater net force and prevent the droplet from penetrating into the mortar surface.[22]

While the self-cleaning property of SM is promising, one of the major problems of superhydrophobic coatings is their poor mechanical durability. Therefore, the mechanical durability of SM was evaluated using water drop impact test, sand abrasion impact test, tape peeling test and sandpaper abrasion test, as shown in Fig. 5a–d and Table II. In the water drop impact test, the WCA of SM decreased to less than 150° after impinging of 10000 water droplets. Additionally,

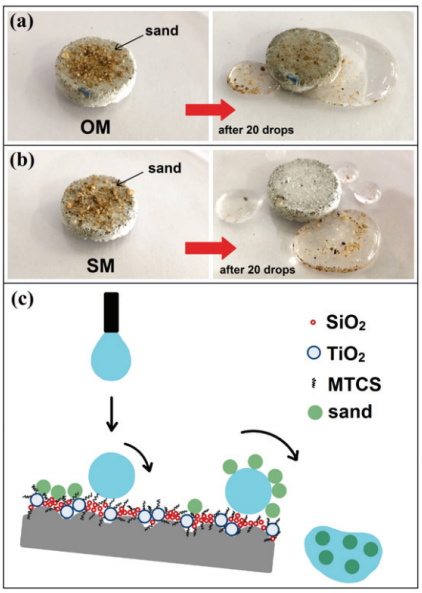

Fig. 4. The self-cleaning test of: a) ordinary mortar, b) superhydrophobic mortar and c) mechanism diagram of self-cleaning.

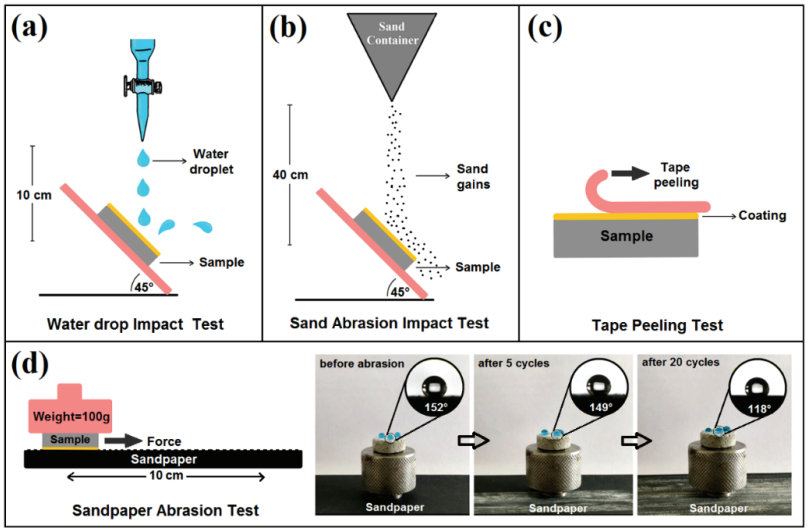

Fig. 5. Schematic of mechanical durability tests: a) water drop impact test, b) sand abrasion impact test, c) tape peeling test and d) sandpaper abrasion test on superhydrophobic mortar.

the sand abrasion impact test was also performed to investigate the durability of the superhydrophobic coating to simulate the impact of dust particles. The SM lost its superhydrophobicity after impingement with 300 g of sand gains. Moreover, the superhydrophobicity of the SM surface was retained even after 60

cycles in the tape peeling test. Fig. 5d shows the sandpaper abrasion test on the SM. Before abrasion, water drops were placed on the SM surface with a WCA of ~152°. After 5 cycles of abrasion, the superhydrophobicity of SM was only slightly reduced. The superhydrophobic coating was robust after dragging nearly 50 cm on the sandpaper, which shows high durability compared to the same experiment set up in the other research.[8] However, the coating surface was severely abraded after 20 cycles (200 cm in length) of abrasion, resulting in a dramatic decrease in WCA to ~118°. Interestingly, the abraded mortar exhibited a significant reduction in water absorption, approximately 82.6 %, compared to OM. These results confirmed the robust superhydrophobic mortar despite the coating being applied only on the surface, which allowed the coating to be used in practical applications on a large-scale.

TABLE II. Mechanical durability tests of superhydrophobic mortar

Water drop impact test		Sand abrasion impact test		Tape peeling test		Sandpaper abrasion test	
Number of drops	WCA / °	Sand gain g	*WCA* / °	Number of cycles	*WCA* / °	Number of cycles	*WCA* / °
0	154±1	0	154±1	0	154±1	0	154±1
10000	149±2	100	151±2	30	150±2	5	149±3
20000	145±1	200	150±3	60	149±2	10	135±4
30000	123±2	300	149±3	90	141±4	15	131±6
40000	115±2	400	140±4	120	131±4	20	118±5

Anti-corrosion analysis

Fig. 6 shows the depth of chloride ion penetration in OM and SM after immersion in NaCl solution for 14 days and subsequent spraying with $AgNO_3$ solution. In the $AgNO_3$ color development test, chloride permeated regions turn violet due to AgCl precipitation, while regions without chloride penetration turn brown due to the formation of Ag_2O.[3,23] The chemical reactions of the $AgNO_3$ color development test are shown in Eqs. (3) and (4):[3]

$$AgNO_3 + NaCl \rightarrow AgCl + NaNO_3 \quad (3)$$

$$2AgNO_3 + 2NaOH \rightarrow Ag_2O + 2NaNO_3 + H_2O \quad (4)$$

The violet regions are affected by the concentration of $AgNO_3$ solution, pH, types of cement and the chloride content of cement.[24] The SM exhibited excellent corrosion resistance, with an average depth of chloride ion penetration of about 1.6 mm (Fig. 6b), while chloride ions were able to penetrate most of the OM (Fig. 6a). Thus, the superhydrophobic coating demonstrated as a good barrier for corrosion and prevents external chloride ions, which are confirmed by the EDS results. The anti-corrosion mortar effectively blocks the diffusion of chloride ions inside the building and might prevent it from reaching the steel inside

the building in chloride salt environments. It was found that the coating method improves the anti-corrosion property of mortar, acting as a protective barrier with effective performance in outdoor and marine environments. The superhydrophobic and anti-corrosion properties prevent water or corrosive ions from entering the mortar, slowing down the corrosion of steel inside the structures and enhancing the durability and service life of construction buildings. Therefore, the fabrication of superhydrophobic mortar can facilitate its durable application in outdoor and marine environments and has the potential as a superhydrophobic coating for various substrates.

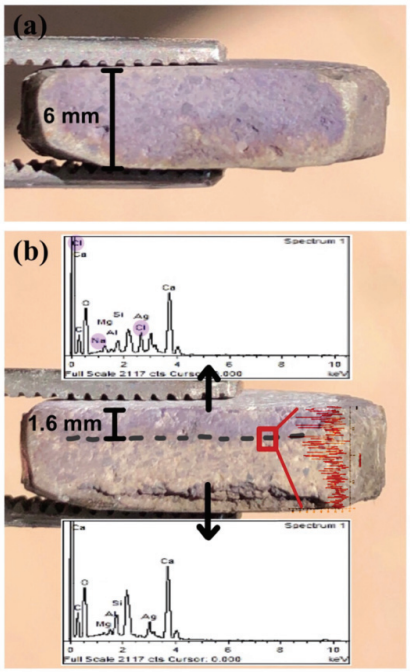

Fig. 6. The chloride ions diffusion of: a) ordinary mortar and b) superhydrophobic mortar obtained by silver nitrate color experiment.

CONCLUSION

In conclusion, the MTCS-modified SiO_2/TiO_2 nanoparticle-coated mortar demonstrates a superhydrophobic surface using a simple spray coating method. A sample coated with a SiO_2/TiO_2 ratio of 75/25 with 15 spraying times exhibits the highest water contact angle and the lowest water absorption with a hierarchical structure. Furthermore, the water absorption of the superhydrophobic mortar was reduced by 97.5 %, indicating excellent waterproofing ability, despite the coating being applied only to the surface. The coated mortars maintained their unique wettability after being impacted with water drop, sand, tape peeling and abraded with sandpaper, demonstrating excellent robustness due to their good mechanical durability properties. Even after being abraded with sandpaper for 20

cycles, the water absorption was reduced by 86.2 %. Moreover, the fabricated superhydrophobic mortar exhibited excellent self-cleaning and anti-corrosion property, effectively reducing chloride ion penetration. Therefore, the simple, cost-effective coating process is suitable for various applications in on-site building construction. In the future, the superhydrophobic coating can be applied to other material surfaces such as wood, metal and plastic to extend their service life.

Acknowledgements. This work was supported by postdoctoral fellowship from the Office of Research Administration, Chiang Mai University, Chiang Mai and The Science Achievement Scholarship of Thailand.

ИЗВОД

ТЕХНОЛОГИЈА НАНОШЕЊА ПРЕВЛАКА НА ПОВРШИНУ МАЛТЕРА ЗА ПРОДУЖЕЊЕ РАДНОГ ВЕКА ГРАЂЕВИНСКИХ КОНСТРУКЦИЈА

NIDCHAMON JUMRUS[1,2], MONWIPA THAPINTA[2], PATCHARAPORN CHAIWONG[2], ARISARA PANTAWAN[1,2], TEWASIN KUMPIKA[2], WINAI THONGPAN[3], NIWAT JHUNTAMA[4], EKKAPONG KANTARAK[2], WATTIKON SROILA[2], RATTIYAKORN RIANYOI[2], PISITH SINGJAI[2] и WIRADEJ THONGSUWAN[2]

[1]Office of Research Administration, Chiang Mai University, Chiang Mai 50200, Thailand, [2]Department of Physics and Materials Science, Faculty of Science, Chiang Mai University, Chiang Mai, 50200, Thailand, [3]Department of Physics, Faculty of Science and Technology, Thammasat University, Lampang, 52190, Thailand и [4]Faculty of Science and Agricultural Technology, Rajamangala University of Technology Lanna, Chiang Mai 50300, Thailand

Суперхидрофобна, самочистећа и антикорозиона превлака је успешно нанета на малтер коришћењем технике једностепеног распршивања. У раствор за распршивање су додате, у различитим односима, наночестице SiO_2 и TiO_2 модификоване метилтрихлоросиланом да би се повећала суперхидрофобност малтера и смањила апсорпција воде. Узорак припремљен при масеном односу SiO_2/TiO_2 = 75/25 је показао највећи контактни угао и најмањи угао клизања, што је обезбедило смањење апсорпције воде веће од 97,5 % и смањење дубине продирања хлоридних јона. Постојаност превлаке је анаизирана различитим тестовима, укључујући утицај падајућих капи воде (10000 капи), абразију песком (300 g), одлепљивање помоћу траке (60 циклуса) и абразију шмиргл папиром (5 циклуса). Превлака је показала одлично смањење апсорпције воде и после теста абразије шмиргл папиром током 20 циклуса (82,6 %), иако је контактни угао смањен на 118°. Приказани резултати указују да формирање суперхидрофобне превлаке на малтеру представља алтернативни приступ, који је једноставан, ефикасан и економичан, за обезбеђење мултифункционалне заштите површине малтера на лицу места у циљу продужења радног века конструкција са побољшаним механичким и антикорозионим својствима.

(Примљено 17. април, ревидирано 24. маја, прихваћено 25. августа 2024)

REFERENCES

1. W. Wang, S. Wang, D. Yao, X. Wang, X. Yu, Y. Zhang, *Constr. Build. Mater*. **238** (2020) 117626 (https://doi.org/10.1016/j.conbuildmat.2019.117626)
2. T. Xiang, J. Liu, Z. Lv, F. Wei, Q. Liu, Y. Zhang, H. Ren, S. Zhou, D. Chen, *Constr. Build. Mater*. **313** (2021) 125482 (https://doi.org/10.1016/j.conbuildmat.2021.125482)
3. L. Qu, Q. Wang, J. Mao, S. Xu, H. Zhang, Z. Shi, X. Li, *Constr. Build. Mater*. **313** (2021) 125540 (https://doi.org/10.1016/j.conbuildmat.2021.125540)

4. N. Jumrus, T. Chaisen, A. Sriboonruang, A. Panthawan, T. Kumpika, E. Kantarak, P. Singjai, W. Thongsuwan, *Mater. Lett.* **264** (2020) 127347 (https://doi.org/10.1016/j.matlet.2020.127347)
5. N. Jumrus, J. Jompaeng, A. Panthawan, T. Kumpika, O. Wiranwetchayan, P. Sanmuangmoon, W. Sroila, E. Kantarak, P. Singjai, W. Thongsuwan, *Mater. Lett*. **304** (2021) 130618 (https://doi.org/10.1016/j.matlet.2021.130618)
6. F. Jiang, T. Zhu, Y. Kuang, H. Wu, S. Li, *Chem. Phys. Lett*. **811** (2023) 140197 (https://doi.org/10.1016/j.cplett.2022.140197)
7. N. Jumrus, N. Suttanon, W. Sroila, P. Tippo, A. Panthawan, W. Thongpan, T. Kumpika, W. Sroila, R. Rianyoi, P. Singjai, W. Thongsuwan, *Mater. Lett*. **330** (2023) 133342 (https://doi.org/10.1016/j.matlet.2022.133342)
8. R. S. Sutar, S. D. Manadeshi, S. S. Latthe, S. R. Kulal, G. D. Salunkhe, K. K. Rangar, R. A. Lavate, S. B. Raut, A. C. Sapkal, A. K. Bhosale, K. K. Sadasivuni, S. Liu, R. Xing, *Macromol. Symp. Spec. Issue:Adv. Mat. Sc. — ICAMS 2020 (Part II)* **393** (2020) 2000033 (http://dx.doi.org/10.1002/masy.202000033)
9. A. Sriboonrung, T. Kumpika, E. Kantarak, W. Sroila, P. Singjai, N. Lawan, S. Muangpil, W. Thongsuwan, *Chiang Mai J. Sci*. **47** (2020) 823-828 (https://epg.science.cmu.ac.th/ejournal/journal-detail.php?id=11108)
10. E. G. Atici, E. Kasapgil, I. Anac, H. Y. Erbil, *Thin Solid Films* **616** (2016) 101 (https://doi.org/10.1016/j.tsf.2016.07.041)
11. K. Pacaphol, D. Aht-Ong, *Surf. Coat. Technol*. **320** (2017) 70 (https://doi.org/10.1016/j.surfcoat.2017.01.111)
12. A. Yu, K.L. Yick, S.P. Ng, J. Yip, Y.F. Chan, *Burns* **46** (2020) 1548 (https://doi.org/10.1016/j.burns.2020.04.014)
13. Z. Yin, M. Xue, Y. Ji, Z. Hong, C. Xie, *Chem. Phys. Lett*. **754** (2020) 137694 (https://doi.org/10.1016/j.cplett.2020.137694)
14. K. Ganesan, K. Rajagopal, K. Thangavel, *Cem. Concr. Compos*. **29** (2007) 515 (https://doi.org/10.1016/j.cemconcomp.2007.03.001)
15. H. Kang, S. Kang, B. Lee, *Materials* **14** (2021) 5407 (https://doi.org/10.3390/ma14185407)
16. C. Yao, A. Xie, Y. Shen, J. Zhu, T. Li, *J. Chil. Chem. Soc*. **58** (2013) 2235 (http://dx.doi.org/10.4067/S0717-97072013000400072)
17. G. Richhariya, D. T. K. Dora, K. R. Parmar, K. K. Pant, N. Singhal, K. Lal, P. P. Kundu, *Materials* **13** (2020) 2921 (https://doi.org/10.3390/ma13132921)
18. J. Wan, L.H. Xu, H. Pan, L.M. Wang, Y. Shen, *J. Porous Mater*. **28** (2021) 1501 (http://dx.doi.org/10.1007/s10934-021-01089-x)
19. G. Semugaza, T. Mielke, M. E. Castillo, A. Gierth, J. X. Tam, S. Nawrath, D. Lupascu, *Mater. Struct.* **56** (2023) 48 (http://dx.doi.org/10.1617/s11527-023-02133-9)
20. R. G. Toro, M. Diab, T. Caro, M. Al-Shemy, A. Adel, D. Caschera, *Materials* **13** (2020) 1326 (https://doi.org/10.3390/ma13061326)
21. J. Li, X. L. Wu, D. S. Hu, Y. M. Yang, T. Qiu, J. C . Shen, *Solid State Commun*. **131** (2004) 21–25 (https://doi.org/10.1016/j.ssc.2004.04.026)
22. Y. Wu, K. Yan, G. Xu, C. Yang, D. Wang, *Prog. Org. Coat.* **159** (2021) 106411 (https://doi.org/10.1016/j.porgcoat.2021.106411)
23. A. R. A. Javier, N. E. Lopez, J. B. P. Juanzon, *Procedia Eng*. **171** (2017) 543 (http://dx.doi.org/10.1016/j.proeng.2017.01.369)
24. L. V. Real, D. R. B. Oliveira, T. Soares, M. H. F. de Medeiros, *Revista ALCONPAT* **5** (2015) 141 (https://dx.doi.org/10.21041/ra.v5i2.84).